

Accepted Manuscript

Structure and properties of layered perovskites $Ba_{1-x}Ln_xFe_{1-y}Co_yO_{3-\delta}$ (Ln = Pr, Sm, Gd)

N.E. Volkova, M. Yu. Mychinko, I.B. Golovachev, A.E. Makarova, M.V. Bazueva, E.I. Zyaikin, L. Ya. Gavrilova, V.A. Cherepanov

PII: S0925-8388(18)34962-4

DOI: <https://doi.org/10.1016/j.jallcom.2018.12.391>

Reference: JALCOM 49034

To appear in: *Journal of Alloys and Compounds*

Received Date: 18 October 2018

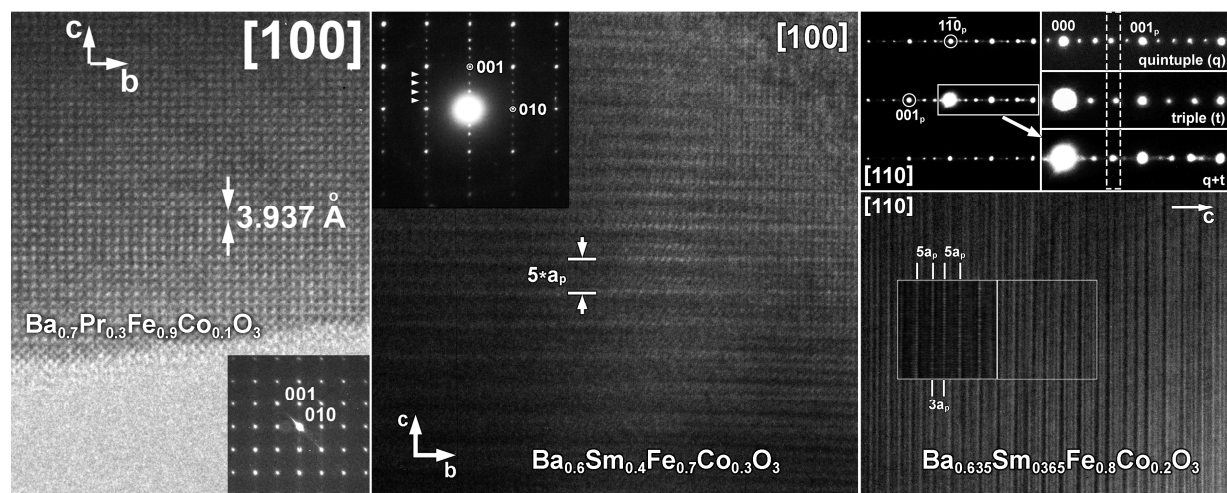
Revised Date: 25 December 2018

Accepted Date: 31 December 2018

Please cite this article as: N.E. Volkova, M.Y. Mychinko, I.B. Golovachev, A.E. Makarova, M.V. Bazueva, E.I. Zyaikin, L.Y. Gavrilova, V.A. Cherepanov, Structure and properties of layered perovskites $Ba_{1-x}Ln_xFe_{1-y}Co_yO_{3-\delta}$ (Ln = Pr, Sm, Gd), *Journal of Alloys and Compounds* (2019), doi: <https://doi.org/10.1016/j.jallcom.2018.12.391>.

This is a PDF file of an unedited manuscript that has been accepted for publication. As a service to our customers we are providing this early version of the manuscript. The manuscript will undergo copyediting, typesetting, and review of the resulting proof before it is published in its final form. Please note that during the production process errors may be discovered which could affect the content, and all legal disclaimers that apply to the journal pertain.







*N.E. Volkova**, *M.Yu. Mychinko*, *I.B. Golovachev*, *A.E. Makarova*, *M.V. Bazueva*,

E.I. Zyaikin, *L.Ya. Gavrilova*, *V.A. Cherepanov*

Institute of Natural Science and Mathematics, Ural Federal University,

Yekaterinburg, Russia

* - corresponding author nadezhda.volkova@urfu.ru

Abstract: A series of samples of overall composition $\text{Ba}_{1-x}\text{Ln}_x\text{Fe}_{1-y}\text{Co}_y\text{O}_{3-\delta}$ (Ln = Pr, Sm, Gd) with $x = 0.3-0.4$; $y = 0-0.5$ were prepared by glycerin nitrate technique in air. The crystal structure of single-phase $\text{Ba}_{1-x}\text{Ln}_x\text{Fe}_{1-y}\text{Co}_y\text{O}_{3-\delta}$ (Ln = Pr, Sm, Gd) determined by XRD was described as cubic (sp. gr. $Pm\bar{3}m$). However, transmission electronic microscopy revealed that both Sm- and Gd-doped oxides possess tetragonal structure with 5-fold and 3-fold increased c parameter respectively. Oxygen content in the complex oxides has been determined in air over wide temperature range by means of thermogravimetry and iodometric titration. The change in oxygen content with temperature for the phases with five-layered ordering was significantly smaller than for the disordered phases.

Keywords: oxide materials, crystal structure, X-ray diffraction, transmission electron microscopy, oxygen nonstoichiometry

1. Introduction

Perovskite oxide materials with the general formula of ABO_3 , where A is alkali earth or rare earth metals and B is transition metal, have attracted much attention as cathodes for solid oxide fuel cells (SOFC) because of their high electronic conductivity and fast mobility of oxygen ions [1-4]. The introduction of Ba^{2+} and Ln^{3+} ions with significantly different radii into the A-sites leads to formation of the layered perovskite-type structures which have formed due to the cations ordering in the alternating layers [5-13]. Depending on the nature of rare earth and $3d$ metal it was possible to obtain double [5-7, 13], triple [9, 10, 12], or quintuple [8, 11] perovskites. Formation of the five-fold layered $\text{Ln}_{2-\varepsilon}\text{Ba}_{3+\varepsilon}\text{Fe}_5\text{O}_{15-\delta}$ phases is possible in the Fe-based systems in air [8, 11, 14]. Such 5-fold layered

structure is formed by alternation of the layers containing exclusively samarium or barium together with the mixed (Sm,Ba) layers along the c-axis: Sm–Ba–(Sm,Ba)–(Sm,Ba)–Ba–Sm [8]. Recent studies revealed that partial substitution of cobalt for iron stabilized quintuple layered structure [14, 15]. In the present work we have shown the effect of rare earth element nature and role of Ln/Ba and Fe/Co ratio for the crystal structure and oxygen content for the $Ba_{1-x}Ln_xFe_{1-y}Co_yO_{3-\delta}$ (Ln = Pr, Sm, Gd; $x = 0.3-0.4$; $y = 0-0.5$) phases.

2. Experimental

The samples of overall composition $Ba_{1-x}Ln_xFe_{1-y}Co_yO_{3-\delta}$ (Ln = Pr, Sm, Gd; $x = 0.3-0.4$; $y = 0.1-0.5$) were prepared using a glycerin nitrate technique. Rare earth oxides (Pr_6O_{11} , Sm_2O_3 and Gd_2O_3) with the purity not less than 99.99%, barium carbonate $BaCO_3$ (99.9%), metallic cobalt Co, iron oxalate $FeC_2O_4 \times 2H_2O$ (99.0%), nitric acid and glycerin were used as the starting materials. Metallic cobalt was obtained by reducing cobalt oxide Co_3O_4 (99.9%) in the hydrogen flow at 400–600°C during 6 h. The appropriate amounts of starting materials were dissolved in 4.5 M nitric acid, and then glycerin was added to the solution. Following heating first led to the formation of viscous gel that subsequently transformed to brown powder. The final annealing was performed at 1100°C in air during 120 h with intermediate grindings, followed by a slow cooling down to room temperature at the rate of about 100°/h. The phase composition of the annealed samples was determined by X-ray diffraction (XRD) using a Shimadzu XRD-7000 instrument (CuK α -radiation, angle range $2\Theta = 20^\circ-90^\circ$, step 0.03°, 5 s/step) in air. The structural parameters were refined by the Rietveld profile method using the Fullprof-2008 package.

SAED and HRTEM images of the single phase samples that were deposited in a form of suspension in ethanol on lacy carbon grids have been collected using a JEOL JEM 2100 and FEI Technai G2 30 UT microscopes operated at 200 and 300 kV respectively.

Thermogravimetric analysis (TGA) was carried out using a STA 409PC instrument (Netzsch) within the temperature range 25–1100 °C. Two measurement

modes were employed, namely: static (10 h dwells at a fixed temperature, with the temperature steps of 25–50°C) and dynamic (continuous heating/cooling rate of 1°C/min). The absolute values of oxygen content were determined by the iodometric titration method described elsewhere [14].

3. Results and discussion

The compositions of single phase oxides which were confirmed by the XRD examination of the studied $\text{Ba}_{1-x}\text{Ln}_x\text{Fe}_{1-y}\text{Co}_y\text{O}_{3-\delta}$ ($\text{Ln} = \text{Pr}, \text{Sm}, \text{Gd}; x = 0.3-0.4; y = 0-0.5$) samples slowly cooled from 1100°C to room temperature are listed in Table 1.

The XRD patterns of all single phase $\text{Ba}_{1-x}\text{Ln}_x\text{Fe}_{1-y}\text{Co}_y\text{O}_{3-\delta}$ samples were refined either by the Rietveld method or by the Le Bail refinement within the cubic structure (space group $Pm\bar{3}m$). Typical XRD patterns for the selected single phase samples are shown in Figure 1. The values of unit cell parameters, unit cell volumes, and R -factors refined from the XRD results for the single phase oxides are listed in Table 2.

It is obvious that concentration of $3d$ metals in the $\text{Ba}_{1-x}\text{Ln}_x\text{Fe}_{1-y}\text{Co}_y\text{O}_{3-\delta}$ phases has no significant effect to the unit cell parameters, which values are consistent with the previously obtained results [14]. In contrast, the values of unit cell parameter noticeably decreased with the decrease of lanthanide ion radii and its content ($r_{\text{Ba}^{2+}}=1.61 \text{ \AA}; r_{\text{Pr}^{3+}}=1.32 \text{ \AA}; r_{\text{Sm}^{3+}}=1.24 \text{ \AA}; r_{\text{Gd}^{3+}}=1.11 \text{ \AA}$ [16]).

It was shown earlier that due to the chemical twinning along the orthogonal directions XRD analysis cannot detect the formation of layered ordered supercell, but electron microscopy required to prove it [8]. Therefore the next step of structural examination was a transmission electron microscopy study.

The detailed TEM study of praseodymium-containing oxides $\text{Ba}_{1-x}\text{Pr}_x\text{Fe}_{1-y}\text{Co}_y\text{O}_{3-\delta}$ confirmed that regardless of Pr/Ba and Fe/Co ratio all oxides possess the ideal cubic perovskite structure with random distribution of Pr and Ba in the A-site positions as well as Fe and Co in the B-site sublattice (Fig. 2).

This result differs the phase relations for rare earth barium ferrites compared to that observed in the related cobaltite systems in air, where formation of layered double perovskites have started from $\text{PrBaCo}_2\text{O}_{6-\delta}$ [5].

A decrease of Ln size drastically changes phase formation. Similarly to the earlier reported $\text{Sm}_{2-\epsilon}\text{Ba}_{3+\epsilon}\text{Fe}_5\text{O}_{14.22}$ [8] and $\text{Sm}_2\text{Ba}_3\text{Fe}_3\text{Co}_2\text{O}_{14.07}$ [14] (the latter formula recalculated to the form of “simple perovskite” by dividing on 5 can be written as $\text{Sm}_{0.4}\text{Ba}_{0.6}\text{Fe}_{0.6}\text{Co}_{0.4}\text{O}_{3-\delta}$) all samples with the intermediate Co-content studied in this work also exhibited a quintuple supercell. The SAED and HRTEM images for $\text{Sm}_2\text{Ba}_3\text{Fe}_{3.5}\text{Co}_{1.5}\text{O}_{15-5\delta}$ ($\text{Sm}_{0.4}\text{Ba}_{0.6}\text{Fe}_{0.7}\text{Co}_{0.3}\text{O}_{3-\delta}$) shown in Fig. 3 illustrate 5-fold ordering and chemical twinning along three cubic directions of the perovskite basic structure. The different brightness of the dots originate because of difference in the scattering factors of different atoms forming correspondent atomic columns reflecting 5-fold alternating of A-site atoms: “Sm – Ba – (Sm,Ba) – (Sm,Ba) – Ba – Sm” [8, 14]. Partial substitution of Co for Fe stabilizes 5-fold superstructure, which can be obtained as for the ideal (2/3) Sm/Ba ratio so for the “nonstoichiometric” $((2-\epsilon)/(3+\epsilon))$ Sm/Ba ratio.

It worth to note that although partial substitution of Co for Fe stabilizes quintuple perovskite structure on the other hand the double perovskite $\text{SmBaCo}_2\text{O}_{6-\delta}$ was found to be stable at 1100°C in air in the $\text{Sm}_2\text{O}_3 - \text{BaO} - \text{CoO}$ system [7]. Moreover, partial substitution of Fe for Co is possible within the double perovskite structure $\text{SmBaCo}_{2-y}\text{Fe}_y\text{O}_{6-\delta}$ up to $y = 1.1$ [17].

Here we can also mentioned that according to our previous works Nd-containing Co-doped ferrites demonstrate intermediate behavior between Pr- and Sm-containing systems in respect to phase formation [11, 15, 18]: the domains of quintuple perovskite were incorporated into the disordered perovskite matrix, Nd/Ba ratio was shown to be a critical factor for the formation of 5-fold structure, Co substitution stabilized the ordered quintuple structure and finally, neodymium barium cobaltite with the double perovskite structure can be partially doped by iron $\text{NdBaCo}_{2-y}\text{Fe}_y\text{O}_{6-\delta}$.

More complicate situation occurs in the Gd-containing system. Earlier it was shown that stabilization of quintuple perovskite structure in the Eu-containing system can be achieved only by Co for Fe partial substitution yielding the formula $\text{Eu}_2\text{Ba}_3\text{Fe}_3\text{Co}_2\text{O}_{13.72}$ [14]. Similar behavior was detected in the Gd-containing system. Co-rich sample of the $\text{Gd}_{0.365}\text{Ba}_{0.635}\text{Fe}_{0.6}\text{Co}_{0.4}\text{O}_{3-\delta}$ composition crystallized in the form of quintuple layered perovskite, so its formula should be written as $\text{Gd}_{1.825}\text{Ba}_{3.175}\text{Fe}_3\text{Co}_2\text{O}_{15.5\delta}$. The ordering of atomic columns with low, medium and high brightness along z axis that obviously observed in the HRTEM image (Fig. 4) confirms electron diffraction data and can be described as “Gd–Ba–Ba,Gd–Ba,Gd–Ba–Gd” alternation of A-site cations in corresponding layers yielding to the formula $\text{Gd}_{2-\varepsilon}\text{Ba}_{3+\varepsilon}\text{Fe}_3\text{Co}_2\text{O}_{15.5\delta}$. However, the SAED and HRTEM images for the sample $\text{Gd}_{0.365}\text{Ba}_{0.625}\text{Fe}_{0.9}\text{Co}_{0.1}\text{O}_{3-\delta}$ with poorest Co content differ significantly. Additional to the simple perovskite structure spots and their relative brightness indicate the formation of so-called triple perovskite (or 123-phase) with the “Gd–Ba–Ba–Gd” alternation of A-site cations (Fig. 5). Taking into account this type of ordering the formula of the $\text{Gd}_{0.365}\text{Ba}_{0.625}\text{Fe}_{0.9}\text{Co}_{0.1}\text{O}_{3-\delta}$ oxide should be written as follows: $\text{Gd}_{1+\varepsilon}\text{Ba}_{2-\varepsilon}\text{Fe}_{2.7}\text{Co}_{0.3}\text{O}_{8+w}$ ($\varepsilon \approx 0.1$).

Since $\text{Ba}_{0.365}\text{Gd}_{0.635}\text{Fe}_{0.9}\text{Co}_{0.1}\text{O}_{3-\delta}$ and $\text{Ba}_{0.365}\text{Gd}_{0.635}\text{Fe}_{0.6}\text{Co}_{0.4}\text{O}_{3-\delta}$ samples should be considered as triple $\text{Gd}_{1+\varepsilon}\text{Ba}_{2-\varepsilon}\text{Fe}_{2.7}\text{Co}_{0.3}\text{O}_{8+w}$ ($\varepsilon \approx 0.1$) and quintuple $\text{Gd}_{2-\varepsilon}\text{Ba}_{3+\varepsilon}\text{Fe}_3\text{Co}_2\text{O}_{15.5\delta}$ ($\varepsilon \approx 0.175$) perovskites respectively, the question arise what is the structure of oxide with a nominal composition in between of them, for example $\text{Ba}_{0.365}\text{Gd}_{0.635}\text{Fe}_{0.8}\text{Co}_{0.2}\text{O}_{3-\delta}$? TEM image for this sample is presented in Fig 6. Electron diffraction pattern taken along [110] zone axis supposed to be the sum of two different diffractions since all additional reflexes have different brightness and positions. Some of these reflexes are more intensive and located in between the positions that are specific for triple and quintuple ordered phases mentioned above, so we assume them as a sum of two closely located reflexes. HRTEM images taken along area selected for electron diffraction shows randomly distributed bright and dark spots along z axis of unit cell which can be considered

as random alternating of the unit cells with triple and quintuple orderings. Therefore the sample with intermediate composition can be treated as intergrowth of triple and quintuple perovskites.

Similarly to a samarium barium double cobaltite corresponding gadolinium-based oxide can also formed Fe-substituted solid solutions $\text{GdBaCo}_{2-y}\text{Fe}_y\text{O}_{6-\delta}$ up to $y=1.0$ [19, 20]

The oxygen content and average oxidation state of the iron and cobalt ions in the $\text{Ba}_{1-x}\text{Ln}_x\text{Fe}_{1-y}\text{Co}_y\text{O}_{3-\delta}$ phases, either slowly cooled to room temperature (calculated from the results of iodometric titration) or those related to 1100°C (obtained from the TGA measurements) are listed in Table 3.

A decrease in the Ln^{3+} size and concentration leads to the decrease of oxygen content and mean oxidation state of $3d$ transition metals. These trends can be explained in terms of the bond energy values: the value of standard enthalpies of formation increasing in the row: GdO (-78.7 kJ/mol); SmO (-135.6 kJ/mol); PrO (-147.7 kJ/mol) [21]. The oxygen content slightly decreases with the raise of cobalt concentration in $\text{Ba}_{1-x}\text{Ln}_x\text{Fe}_{1-y}\text{Co}_y\text{O}_{3-\delta}$. This can be understood considering the fact that cobalt is more electronegative compared to iron ($\chi_{\text{Fe}}=1.64$; $\chi_{\text{Co}}=1.7$ according to the Allred and Rochow scale [22]). Therefore cobalt acts as acceptor of electrons (Co'_{Fe}), enhancing formation of oxygen vacancies (v_o''). Concentration dependencies of mean oxidation state for $3d$ -transition metals (iron and cobalt) in $\text{Ba}_{1-x}\text{Ln}_x\text{Fe}_{1-y}\text{Co}_y\text{O}_{3-\delta}$ are presented in Fig. 7.

Raw experimental results of TGA measurements for $\text{Ba}_{1-x}\text{Ln}_x\text{Fe}_{1-y}\text{Co}_y\text{O}_{3-\delta}$, vs. temperature in air obtained in the dynamic mode with the cooling/heating rate $1^\circ/\text{min}$ (shown by the lines) and obtained in the static mode (isothermal dwells at each temperature shown by points), nicely coincided with each other, which confirms fast oxygen release/uptake kinetics (see Fig. S1 in the Supplementary file). Taking into account the absolute values of oxygen content extracted from the results of iodometric titration the values of $(3 - \delta)$ were calculated from the TG result within the entire temperature range (Fig. 8).

The largest change in oxygen content has been found for the disordered perovskites. The triple and quintuple perovskites exhibited much smaller variation in oxygen content. This is consistent with the observation for the quintuple perovskites about predominant location of oxygen vacancies between the mixed (Sm,Ba) layers [8].

4. Conclusion

The present study have shown that crystal chemistry of oxide systems containing rare earth elements (Pr, Sm, Gd), Ba and 3d-transition metals (Fe, Co) at fixed conditions (1100°C, air) is complicate and strongly depended on cation's nature and their ratio in A-site (Ln/Ba) and B-site (Fe/Co) positions. Pr-containing system reveals the formation of disordered perovskite structure, while samarium barium ferrites exhibited a formation of quintuple layered structure. Depending on Ln/Ba ratio, Gd-containing system reveals a formation of triple or quintuple perovskite structure.

Acknowledgements

This work was supported in part by the Russian Science Foundation (Grant № 18-73-00159) and the Russian Foundation for Basic Research (Grant № 18-33-00822 mol_a).

References

1. H.Y. Tu, Y. Takeda, N. Imanishi, O. Yamamoto, $\text{Ln}_{1-x}\text{Sr}_x\text{CoO}_3$ (Ln = Sm, Dy) for the electrode of solid oxide fuel cells, *Solid State Ionics*. 100 (3–4) (1997) 283–288. [https://doi.org/10.1016/S0167-2738\(97\)00360-3](https://doi.org/10.1016/S0167-2738(97)00360-3).
2. E.V. Tsipis, V.V. Kharton, Electrode materials and reaction mechanisms in solid oxide fuel cells: a brief review, *J. Solid State Electrochem*. 12 (11) (2008) 1367–1391. <https://doi.org/10.1007/s10008-008-0611-6>.
3. J.-H. Kim, A. J. Manthiram, $\text{LnBaCo}_2\text{O}_{5+d}$ oxides as cathodes for intermediate-temperature solid oxide fuel cells, *Electrochem. Soc.* 155 (2008) B385–390. DOI: 10.1149/1.2839028.

4. A. Tarascón, S.J. Skinner, R.J. Chater, F. Hernández-Ramírez, J.A. Kilner, Layered perovskites as promising cathodes for intermediate temperature solid oxide fuel cells, *J. Mater. Chem.* 17 (2007) 3175–3181. DOI:10.1039/B704320A.
5. A. Maignan, C. Martin, D. Pelloquin, N. Nguyen, B. Raveau, Structural and Magnetic Studies of Ordered Oxygen-Deficient Perovskites $\text{LnBaCo}_2\text{O}_{5+\delta}$, Closely Related to the “112” Structure, *J. Solid State Chem.* 142 (1999) 247–260. DOI: 10.1006/jssc.1998.7934.
6. P.S. Anderson, C.A. Kirk, J. Knudsen, I.M. Reaney, A.R. West, Structural characterisation of $\text{REBaCo}_2\text{O}_{6-\delta}$ phases (RE = Pr, Nd, Sm, Eu, Gd, Tb, Dy, Ho), *Solid State Sci.* 7 (2005) 1149–1156. DOI: 10.1016/j.solidstatesciences.2005.03.004.
7. L.Ya. Gavrilova, T.V. Aksenova, N.E. Volkova, A.S. Podzorova, V.A. Cherepanov, Phase equilibria and crystal structure of the complex oxides in the Ln–Ba–Co–O (Ln=Nd, Sm) systems, *J. Solid State Chem.* 184 (2011) 2083–2087. DOI: 10.1016/j.jssc.2011.06.006.
8. N.E. Volkova, O.I. Lebedev, L.Ya. Gavrilova, S. Turner, N. Gauquelin, Md. M. Seikh, V. Caignaert, V.A. Cherepanov, B. Raveau, G. Van Tendeloo, Nanoscale Ordering in Oxygen Deficient Quintuple Perovskite $\text{Sm}_{2\bar{6}}\text{Ba}_{3+\delta}\text{Fe}_5\text{O}_{15\bar{6}}$: Implication for Magnetism and Oxygen Stoichiometry, *Chem. Mater.* 26 (2014) 6303–6310. DOI: 10.1021/cm503276p.
9. J. Linden, P. Karen, A. Kjekshus, J. Miettinen, M. Karppinen, Partial Oxygen Ordering in Cubic Perovskite $\text{REBa}_2\text{Fe}_3\text{O}_{8+w}$ (RE=Gd, Eu, Sm, Nd), *J. Solid State Chem.* 144 (1999) 398–404. <https://doi.org/10.1006/jssc.1999.8178>.
10. P. Karen, A. Kjekshus, Q. Huang, J. W. Lynn, N. Rosov, I. Natali Sora, V.L. Karen, A.D. Mighell, A. Santoro Neutron powder diffraction study of nuclear and magnetic structures of oxidized and reduced $\text{YBa}_2\text{Fe}_3\text{O}_{8+w}$, *J. Solid State Chem.* 174 (2003) 87–95. [https://doi.org/10.1016/S0022-4596\(03\)00180-4](https://doi.org/10.1016/S0022-4596(03)00180-4).
- 11 N.E. Volkova, A.S. Urusova, L.Ya. Gavrilova, A.V. Bryuzgina, K.M. Deryabina, M.Yu. Mychinko, O.I. Lebedev, B. Raveau, V.A. Cherepanov, Special

Features of Phase Equilibriums in Ln–Ba–Fe–O Systems, *Russ. J. Gen. Chem.*, 86 (8) (2016) 1800–1804. DOI: 10.1134/S1070363216080041.

12. B. Raveau, C. Michel, M. Hervieu, D. Groult, *Crystal Chemistry of High-Tc Superconducting Copper Oxides*, Springer Verlag, 1991.

13. T.V. Aksenova, L.Ya. Gavrilova, D.S. Tsvetkov, V.I. Voronin, V.A. Cherepanov, *Crystal Structure and Physicochemical Properties of Layered Perovskite-Like Phases $\text{LnBaCo}_2\text{O}_{5+\delta}$* , *Russian Journal of Physical Chemistry A*, 85 (3) (2011) 427–432. DOI: 10.1134/S0036024411030022.

14. A.K. Kundu, O.I. Lebedev, N.E. Volkova, Md.M. Seikh, V. Caignaert, V.A. Cherepanov, B. Raveau, Quintuple perovskites $\text{Ln}_2\text{Ba}_3\text{Fe}_{5-x}\text{Co}_x\text{O}_{15-d}$ (Ln = Sm, Eu): nanoscale ordering and unconventional magnetism, *J. Mater. Chem. C* 3 (2015) 5398–5405. DOI: 10.1039/c5tc00494b.

15. A.K. Kundu, M.Yu. Mychinko, V. Caignaert, O.I. Lebedev, N.E. Volkova, K.M. Deryabina, V.A. Cherepanov, B. Raveau, Coherent inter growth of simple cubic and quintuple tetragonal perovskites in the system $\text{Nd}_{2-\epsilon}\text{Ba}_{3+\epsilon}(\text{Fe},\text{Co})_5\text{O}_{15-\delta}$, *J. Solid State Chem.* 231 (2015) 36–41. <http://dx.doi.org/10.1016/j.jssc.2015.07.050>.

16. R.D. Shannon, Revised effective ionic radii and systematic studies of interatomic distances in halides and chalcogenides, *Acta Cryst. A* 32 (1976) 751–767.

17. N.E. Volkova, L.Ya. Gavrilova, V.A. Cherepanov, T.V. Aksenova, V.A. Kolotygin, V.V. Kharton, Synthesis, crystal structure and properties of $\text{SmBaCo}_{2-x}\text{Fe}_x\text{O}_{5+\delta}$, *J. Solid State Chem.* 204 (2013) 219–223. <http://dx.doi.org/10.1016/j.jssc.2013.06.001>.

18. V.A. Cherepanov, T.V. Aksenova, L.Ya. Gavrilova, K.N. Mikhaleva, Structure, nonstoichiometry and thermal expansion of the $\text{NdBa}(\text{Co},\text{Fe})_2\text{O}_{5+\delta}$ layered perovskite, *Solid State Ionics*. 188 (1) (2011) 53–57. DOI: 10.1016/j.ssi.2010.10.021.

19. D.S. Tsvetkov, I.L. Ivanov, A.Yu. Zuev, Crystal structure and oxygen content of the double perovskites $\text{GdBaCo}_{2-x}\text{Fe}_x\text{O}_{6-\delta}$, *J. Solid State Chem.* 199 (2013) 154–159. <https://doi.org/10.1016/j.jssc.2012.12.013>.

20. Y.N. Kim, J.-H. Kim, A. Manthiram, Effect of Fe substitution on the structure and properties of $\text{LnBaCo}_{2-x}\text{Fe}_x\text{O}_{5+\delta}$ (Ln =Nd and Gd) cathodes, *J. Power Sources*. 195 (19) (2010) 6411–6419. <https://doi.org/10.1016/j.jpowsour.2010.03.100>.
21. S.P. Gordienko, B.V. Fenochka, G.Sh. Viksman Thermodynamics of lanthanide compounds, Naukova Dumka, Kiev, 1979.
22. J.E. Huheey, *Inorganic Chemistry*, Harper&Row, NewYork, 1983.

Table 1 – The compositions of the single phase $\text{Ba}_{1-x}\text{Ln}_x\text{Fe}_{1-y}\text{Co}_y\text{O}_{3-\delta}$ (Ln = Pr, Sm, Gd) samples

Ln	x	y
Pr	0.3	0.1-0.5
	0.4	0.1-0.3
Sm	0.4	0.1-0.3
Gd	0.365	0.1-0.4

Table 2 – Unit cell parameters of $\text{Ba}_{1-x}\text{Ln}_x\text{Fe}_{1-y}\text{Co}_y\text{O}_{3-\delta}$ (Ln = Pr, Sm, Gd) and relevant agreement factors extracted from the Le Bail refinement (*) or the Rietveld refinement results (**)

Ln	x	y	$a, \text{\AA}$	$V, \text{\AA}^3$	$R_{Br}, \%$	$R_f, \%$
Pr	0.3	0.1	3.961(1)	62.14(2)	0.706*	0.734*
		0.2	3.952(1)	61.72(2)	0.642*	0.638*
		0.3	3.952(1)	61.72(1)	5.96**	3.94**
		0.4	3.952(1)	61.72(2)	1.67*	1.15*
		0.5	3.954(1)	61.82(2)	0.566*	0.446*
	0.4	0.1	3.934(1)	60.88(2)	3.81**	2.34**
		0.2	3.929(1)	60.65(2)	1.49*	1.01*
		0.3	3.928(1)	60.60(2)	3.83**	2.67**
Sm	0.4	0.1	3.928(1)	60.61(2)	0.621*	0.795*
		0.2	3.926(1)	60.51(2)	0.801*	0.765*
		0.3	3.924(1)	60.42(2)	0.529*	0.449*
Gd	0.365	0.1	3.927(1)	60.55(2)	1.19*	1.16*
		0.2	3.927(1)	60.55(2)	0.765*	0.712*
		0.3	3.925(1)	60.46(2)	0.989*	0.940*
		0.4	3.924(1)	60.42(2)	0.518*	0.502*

Table 3 – Oxygen content ($3-\delta$), mean oxidation state of iron and cobalt (n_{Me}) ions in $\text{Ba}_{1-x}\text{Ln}_x\text{Fe}_{1-y}\text{Co}_y\text{O}_{3-\delta}$ at 25 and 1100°C.

<i>Ln</i>	<i>x</i>	<i>y</i>	$3-\delta$ (25°C)	n_{Me} (25°C)	$3-\delta$ (1100°C)	n_{Me} (1100°C)
Pr	0.3	0.1	2.89±0.04	3.48	2.74±0.04	3.17
		0.2	2.85±0.04	3.39	2.70±0.04	3.09
		0.3	2.83±0.04	3.36	2.66±0.04	3.03
	0.4	0.1	2.90±0.04	3.40	–	–
		0.2	2.88±0.04	3.35	–	–
		0.3	2.86±0.04	3.31	–	–
Sm	0.4	0.1	2.76±0.04	3.12	–	–
		0.2	2.75±0.04	3.10	2.65±0.04	2.90
		0.3	2.74±0.04	3.08	–	–
Gd	0.365	0.1	2.71±0.04	3.06	2.70±0.04	3.02

Figure 1 – X-ray diffraction patterns of $\text{Ba}_{1-x}\text{Ln}_x\text{Fe}_{1-y}\text{Co}_y\text{O}_{3-\delta}$

Fig. 2 – SAED image taken along [001] [111] and [110] zones axis for $\text{Ba}_{0.7}\text{Pr}_{0.3}\text{Fe}_{0.7}\text{Co}_{0.3}\text{O}_{3-\delta}$

Fig. 3 – HRTEM image for $\text{Sm}_2\text{Ba}_3\text{Fe}_{3.5}\text{Co}_{1.5}\text{O}_{15-5\delta}$ taken along [100] axis (corresponding SAED pattern as inset)

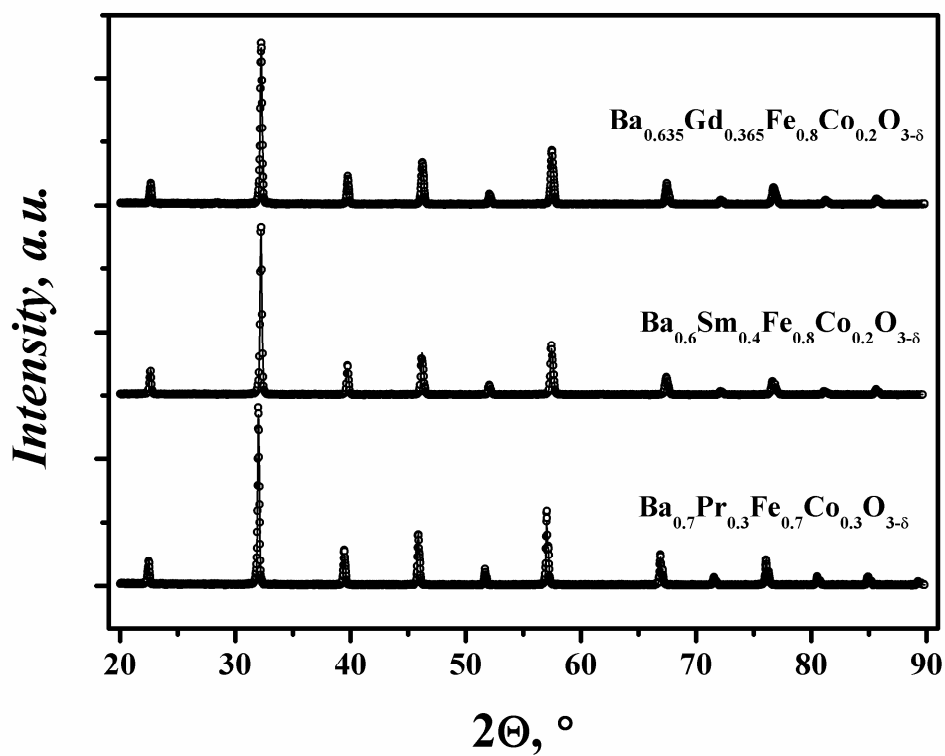
Fig. 4 – SAED images of $\text{Gd}_{0.365}\text{Ba}_{0.635}\text{Fe}_{0.6}\text{Co}_{0.4}\text{O}_{3-\delta}$ taken along (a) [100], (b) [001], (c) [110] and (d, c) HRTEM images taken along [100] zone axis (intensity profile line along z axis as inset)

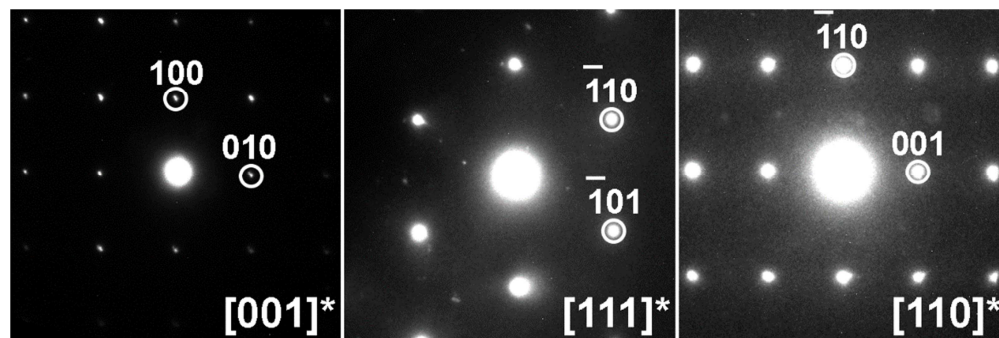
Fig. 5 – HRTEM image of $\text{Gd}_{0.365}\text{Ba}_{0.635}\text{Fe}_{0.9}\text{Co}_{0.1}\text{O}_{3-\delta}$ taken along [100] zone axis (corresponding SAED pattern as inset)

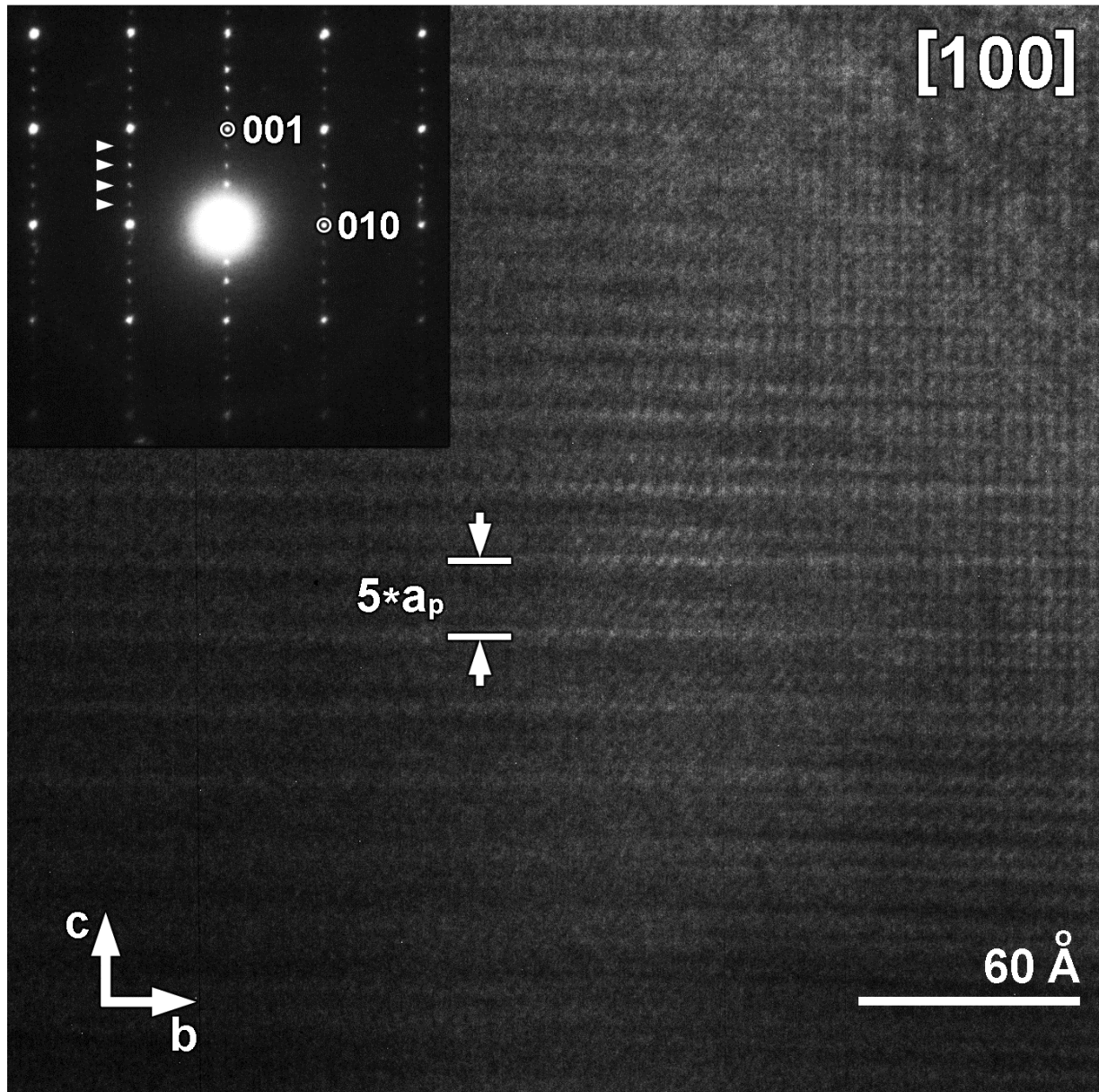
Fig. 6 – SAED image of $\text{Gd}_{0.365}\text{Ba}_{0.635}\text{Fe}_{0.8}\text{Co}_{0.2}\text{O}_{3-\delta}$ taken along (a) [100], (b) comparison of obtained reflexes with different type of orderings, (c) HRTEM image taken along [110] zone axis

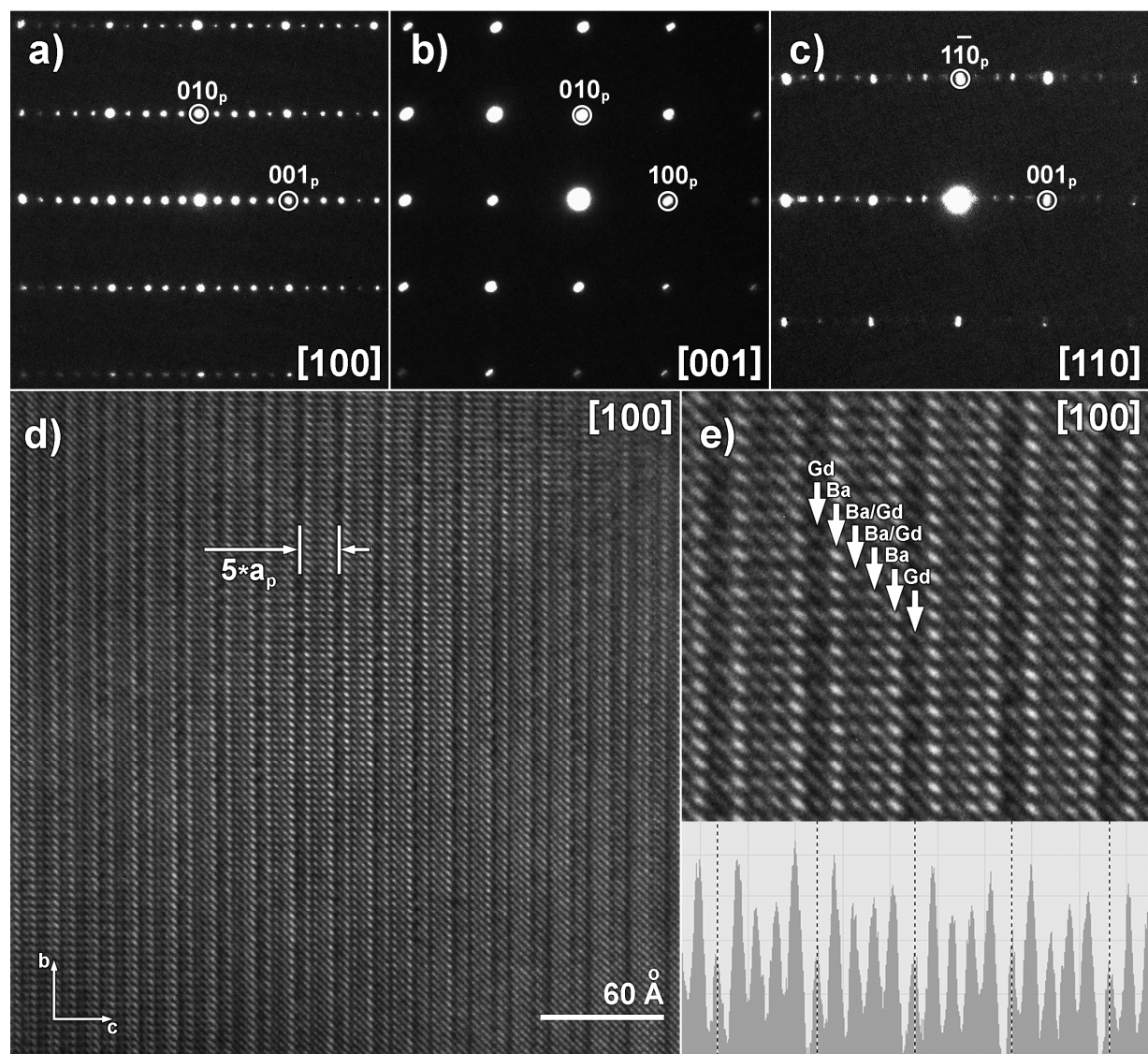
Fig. 7 – The mean oxidation state of 3d-transition metals (iron and cobalt) vs. lanthanide concentration (x) in $\text{Ba}_{1-x}\text{Ln}_x\text{Fe}_{1-y}\text{Co}_y\text{O}_{3-\delta}$ (Ln = Pr, Sm, Gd) at 25 °C in air.

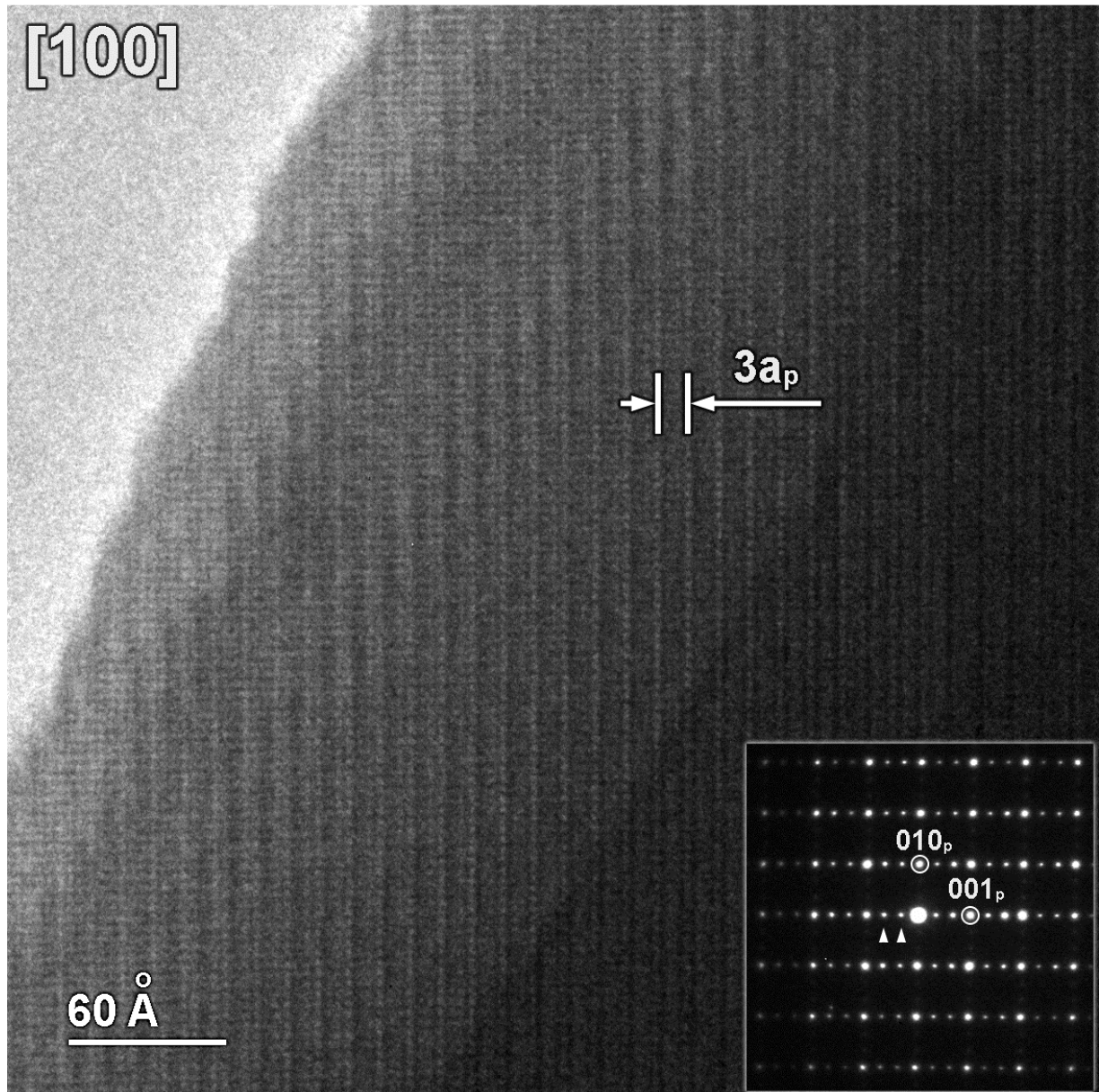
Fig. 8 – Temperature dependencies of oxygen content in $\text{Ba}_{1-x}\text{Ln}_x\text{Fe}_{1-y}\text{Co}_y\text{O}_{3-\delta}$ (Ln = Pr, Sm, Gd) at atmospheric oxygen pressure.

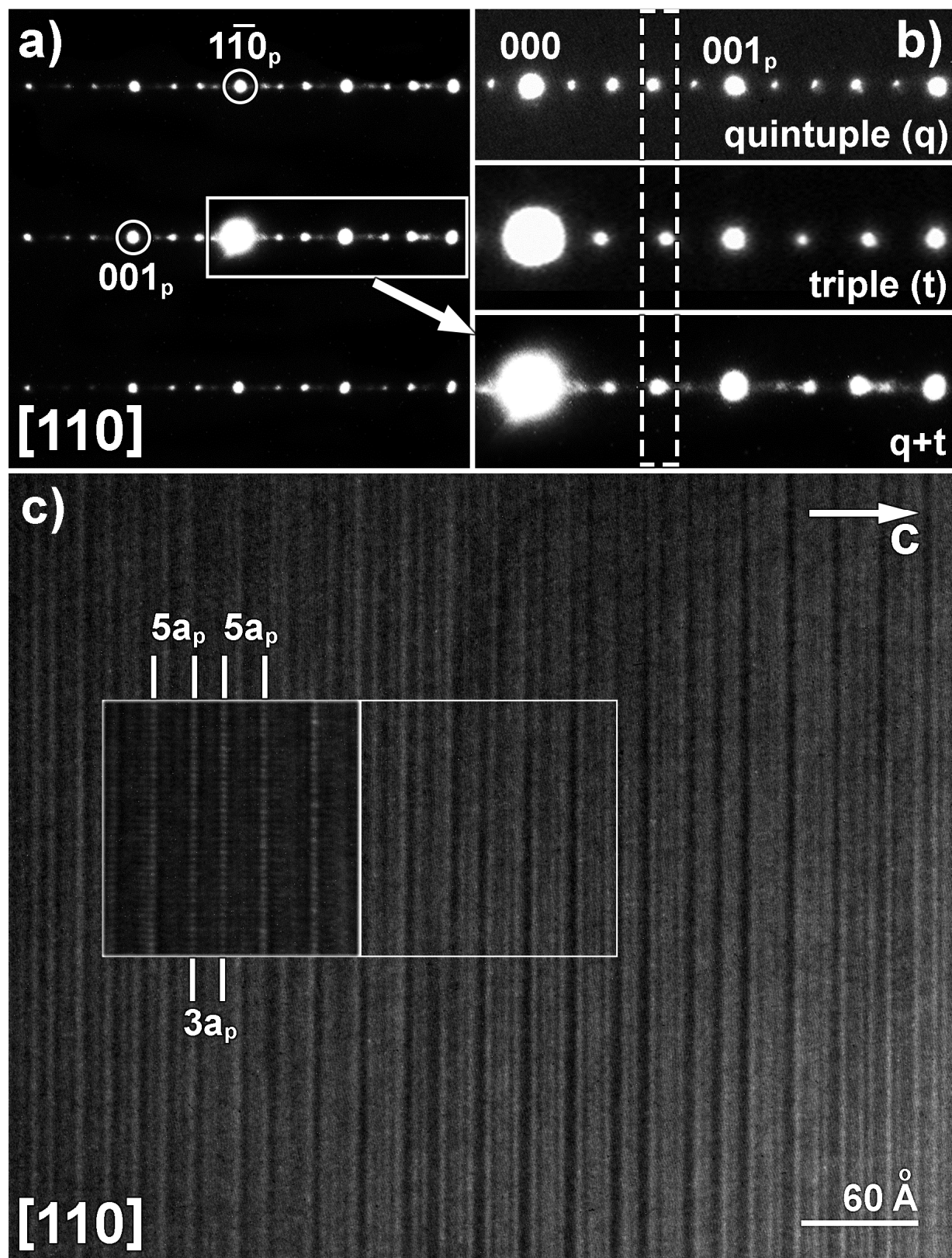


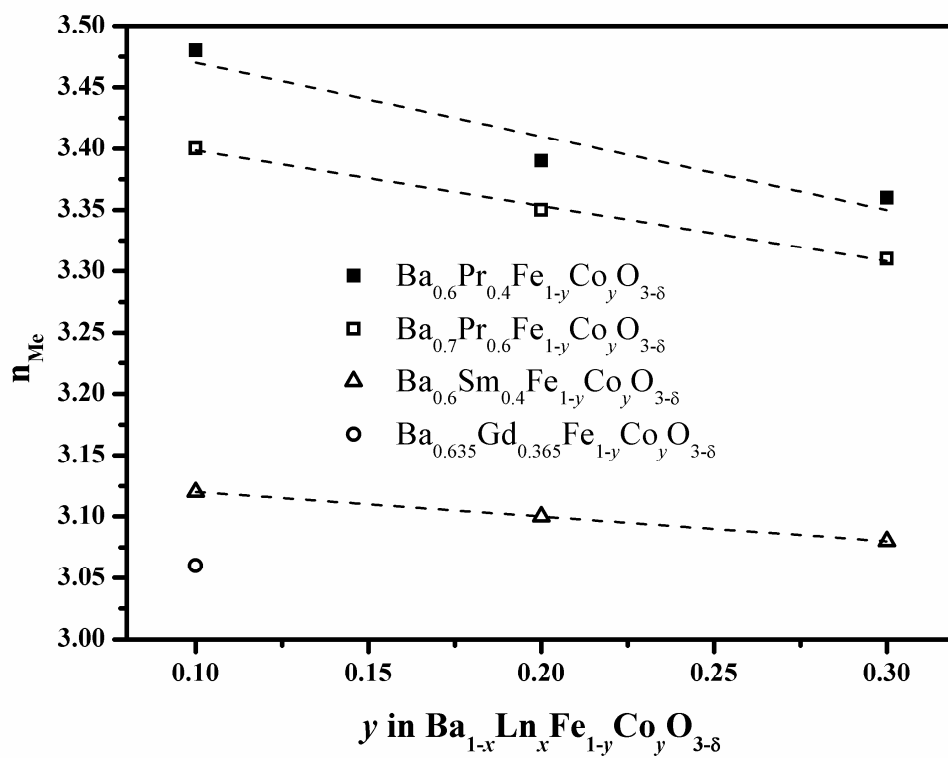


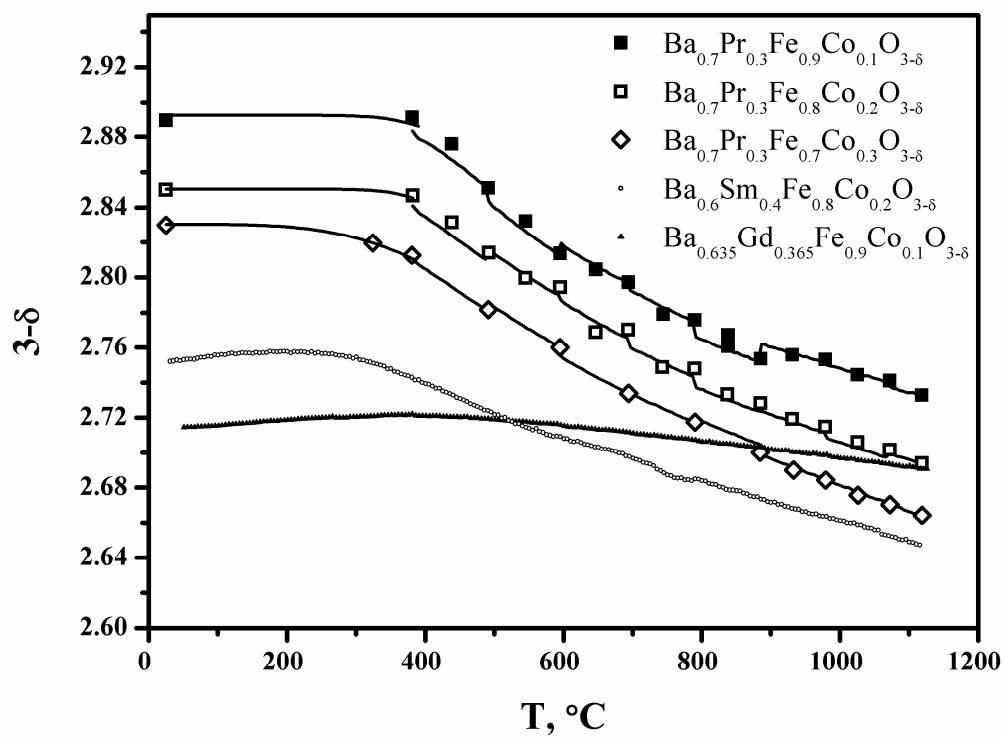












The $\text{Ba}_{1-x}\text{Ln}_x\text{Fe}_{1-y}\text{Co}_y\text{O}_{3-\delta}$ oxides have been prepared by glycerol-nitrate technique;
The homogeneity ranges for the $\text{Ba}_{1-x}\text{Ln}_x\text{Fe}_{1-y}\text{Co}_y\text{O}_{3-\delta}$ solid solutions were determined;
Crystal structure for the $\text{Ba}_{1-x}\text{Ln}_x\text{Fe}_{1-y}\text{Co}_y\text{O}_{3-\delta}$ solid solutions was revealed;
The temperature dependencies of oxygen content in $\text{Ba}_{1-x}\text{Ln}_x\text{Fe}_{1-y}\text{Co}_y\text{O}_{3-\delta}$ were determined.

ACCEPTED MANUSCRIPT